CEP162 is an axoneme-recognition protein promoting ciliary transition zone assembly at the cilia base

Citation	Wang, Won-Jing, Hwee Goon Tay, Rajesh Soni, Geoffrey S. Perumal, Mary G. Goll, Frank P. Macaluso, John M. Asara, Jeffrey D. Amack, and Meng-Fu Bryan Tsou. 2013. "CEP162 is an axoneme-recognition protein promoting ciliary transition zone assembly at the cilia base." Nature cell biology 15 (6): 10.1038/ncb2739. doi:10.1038/ncb2739. http://dx.doi.org/10.1038/ncb2739.
Published Version	doi:10.1038/ncb2739
Accessed	April 17, 2018 4:42:55 PM EDT
Citable Link	http://nrs.harvard.edu/urn-3:HUL.InstRepos:11879412
Terms of Use	This article was downloaded from Harvard University's DASH repository, and is made available under the terms and conditions applicable to Other Posted Material, as set forth at http://nrs.harvard.edu/urn-3:HUL.InstRepos:dash.current.terms-of-use#LAA

(Article begins on next page)

CEP162 is an axoneme-recognition protein promoting ciliary transition zone assembly at the cilia base

Won-Jing Wang[1], **Hwee Goon Tay**[2], **Rajesh Soni**[1], **Geoffrey S. Perumal**[3], **Mary G. Goll**[4], **Frank P. Macaluso**[3], **John M. Asara**[5,6], **Jeffrey D. Amack**[2], and **Meng-Fu Bryan Tsou**[1,7,8]

[1]Cell Biology Program, Memorial Sloan-Kettering Cancer Center, New York, NY 10065

[2]Department of Cell and Developmental Biology, State University of New York, Upstate Medical University, Syracuse, NY 13210

[3]Analytical Imaging Facility, Albert Einstein College of Medicine, Bronx, NY 10461

[4]Developmental Biology Program, Memorial Sloan-Kettering Cancer Center, New York, NY 10065

[5]Department of Medicine, Harvard Medical School, Beth Israel Deaconess Medical Center, Boston, MA, 02115

[6]Mass Spectrometry Core, Beth Israel Deaconess Medical Center, Boston, MA, 02115

[7]Weill Cornell Graduate School of Medical Sciences, Cornell University, New York, NY 10065

Abstract

The transition zone (TZ) is a specialized compartment found at the base of cilia, adjacent to the centriole distal end, where axonemal microtubules (MTs) are heavily cross-linked to the surrounding membrane to form a barrier that gates the ciliary compartment. A number of ciliopathy molecules have been found to associate with the TZ, but factors that directly recognize axonemal MTs to specify TZ assembly at the cilia base remain unclear. Here, through quantitative centrosome proteomics, we identified an axoneme-associated protein, CEP162, tethered specifically at centriole distal ends to promote TZ assembly. CEP162 interacts with core TZ components, and mediates their association with MTs. Loss of CEP162 arrests ciliogenesis at the stage of TZ assembly. Abolishing its centriolar tethering, however, allows CEP162 to stay on the growing end of the axoneme, and ectopically assemble TZ components at cilia tips. This generates extra-long cilia with strikingly swollen tips that actively release ciliary contents into the extracellular environment. CEP162 is thus an axoneme-recognition protein "pre-tethered" at centriole distal ends prior to ciliogenesis to promote and restrict TZ formation specifically at the cilia base.

Introduction

The primary cilium is a membrane-bound, microtubule-based sensory organelle, composed of 9 doublet microtubules (MTs), the axoneme, nucleated directly from the distal end of

centrioles or basal bodies[1, 2]. Primary cilia can sense a wide range of signals in the extracellular surroundings, and thus critically regulate the physiology of cells during proliferation and morphogenesis[3].

In vertebrate cells, cilia biogenesis follows a series of stereotyped steps[1, 2, 4]. Through the distal end, centrioles first interact with small membrane vesicles of unclear specificity, mediated by a set of accessory structures known as the distal appendages[5, 6]. This interaction facilitates the nucleation of short doublet MTs from the centriole distal end[6]. Nascent doublet MTs adjacent to the centriole distal end are heavily cross-linked to the surrounding membrane to form a specialized compartment described as the transition zone (TZ)[7]. MT-to-membrane connections in the TZ can be seen under electron microscopy (EM) as multiple rows of Y-shaped linkers[7] that form a unique organization termed the "ciliary necklace"[7]. After TZ formation, the development of a full-length, mature axoneme (or cilium) is supported and maintained by the intraflagellar transport (IFT) machinery[8, 9].

The TZ has been shown to form a barrier or part of the ciliary gate that works together with the septin ring[10], nucleoporins[11], and likely distal appendages[12] to regulate selective targeting and sorting of proteins to and from the ciliary compartment[13, 14]. Several multiprotein complexes, including NPHP1-4-8[15, 16], MKS/B9[13, 15, 17], and CEP290/NPHP5[15] complexes have been found to associate with the TZ, and many of them are ciliopathy molecules that critically regulate not only cilia biogenesis but also the activity of cilia as a sensory organelle[13, 15–20]. While a large number of TZ components have been discovered[19], how ciliary MTs (or axonemes) are recognized to form the TZ, and how TZ assembly is limited to the cilia base during axoneme elongation remain largely unclear.

Results

Identification of the centriole-distal-end protein CEP162 that binds microtubules

The centriole distal end marks the base of cilia, and is immediately adjacent to the TZ. To identify factors that promote and/or specify TZ formation at the cilia base, we screened for centriole-distal-end proteins that possess microtubule-binding activities. A proteomic approach was designed to quantitatively differentiate core centriolar proteins from other centrosomal components (Fig. 1a) (see Methods for details). We have previously found that centriole duplication in S and G2 phases generates engaged centriole pairs consisting of one modified (mother) centriole that is MTOC competent, and one unmodified (daughter) centriole that is MTOC non-competent[21]. Since only the modified centriole can acquire accessory structures like the pericentriolar material (PCM) and appendages[21] (Fig. 1a), an increase in the number of unmodified centrioles within a centrosome would not change the total amount of accessory proteins in that centrosome. However, an increase in centriolar proteins would occur proportionally. Such differences can be quantitatively detected and analyzed by SILAC (stable isotope labeling by amino acids in cell culture) mass spectrometry[22], and has recently been used to successfully isolate distal appendage proteins[6] associating with modified centrioles (Fig. 1a; 1:1 ratio). Here, the same proteomics tool was used to specifically identify core centriolar proteins present equally in both modified and unmodified centrioles (Fig. 1a; 6:2 ratio). Candidate core centriolar proteins were further examined for their subcellular localization. Nine centriole-distal-end proteins were identified so far, including six previously described proteins: CP110, CEP97, CEP76, Ofd1, CEP290, and SDCCAG8[23–27], and three largely uncharacterized proteins: MPP9, KIAA1009/QN1, and CCHCR1[28, 29]. Among the uncharacterized, KIAA1009 exhibits MT-binding activity (Fig. 1), and thus was further examined.

KIAA1009/QN1, now renamed CEP162, was found in organisms ranging from trypanosomes to vertebrates. It localizes to the distal end of centrioles throughout the cell

cycle (Fig. 1b), co-localizing with the known distal-end marker CP110[23] but not with the proximal-end markers C-Nap1[30] or SAS6 (Fig. 1c). During ciliogenesis, the CEP162 signal became disk-shaped, and was found at the cilia base surrounded by the distal appendage protein CEP164[31] (Fig. 1d), suggesting an intimate association with the axoneme. Consistently, CEP162 was found on spindle MTs in mitosis (Fig. 1e), suggesting that it may possess MT-binding activity. Full-length CEP162 (FL; 1–1403 a.a.) contains 3 coiled-coil (CC) stretches in the C-terminal region: CC1 (617–906 a.a.), CC2 (957–1121 a.a.), and CC3 (1167–1386 a.a.) (Fig. 1f). Deletion of CC3 (CC3 or tNC1C2) abolished centriole localization without affecting MT association (Fig. 1f & h). Conversely, a fragment containing CC2 and CC3 (C2C3) localized to centrioles at distal ends, but failed to associate with MTs (Fig. 1f & g), indicating that the two targeting activities of CEP162 are separable. To test if CEP162 binds directly to MTs, a microtubule-pelleting assay was used. Endogenous CEP162 in cell lysates (Fig. 1i) or a MT-binding fragment of CEP162 (tNC1C2) purified from *E. coli* (Fig. 1j), but not a control fragment (CEP162[1–227]), could be co-pelleted with pure, taxol-stabilized MTs (Fig. 1k), demonstrating that CEP162 binds directly to MTs. Furthermore, overexpression of CEP162[tNC1C2] in cells induced a large number of MT bundles that were insensitive to cold treatment (Fig. 1l).

CEP162 is required for ciliogenesis

To determine the function of CEP162, the protein was depleted from cells by RNAi (Fig. 2 & 3). Unlike a previous report[29], neither mitosis nor centriole duplication were affected by CEP162 depletion (Fig. 2a & b). However, in the absence of CEP162, ciliogenesis was specifically disrupted in retinal pigment epithelial (RPE1) cells (Fig. 2c–e). In vivo studies using zebrafish indicated that the zebrafish CEP162 homolog is maternally supplied and ubiquitously expressed during early embryonic development (Fig. 2f). Partial knockdown of zebrafish Cep162 using antisense morpholino oligonucleotides (MO) results in a series of phenotypes known to associate with cilia defects, including body curvature, hydrocephalus, and left-right asymmetry defects (Fig. 2g–k), which could be partially rescued by expressing RNAi-resistant form of CEP162 (Fig. 2j & k).

Loss of CEP162 arrests ciliogenesis at the stage of TZ assembly

Interestingly, the acquisition of distal appendages (Fig. 3a), the removal of CP110 from the mature centriole[23] (Fig. 3b), and the localization of a known centriole-distal-end protein Ofd1[24] (Fig. 3c) all occurred normally in the absence of CEP162. Moreover, several non-membrane bound TZ components including IFT88, Tctn1, and Cc2d2a, were recruited normally to CEP162-deficient centrioles (Fig. 3d–f), indicating that although cilia fail to form, some early steps of ciliogenesis can proceed without CEP162.

Electron microscopy (EM) was used to examine the ciliogenesis defect in more detail (Fig. 3g). In wild-type cells, more than 88% of mature centrioles (30 out of 34) in G0/G1-arrested cells, judged by the appearance of appendages, efficiently dock to vesicle membranes and support the formation of axoneme or ciliary MTs known to organize the TZ (Fig. 3g, left). Note that by establishing connections alongside the ciliary MTs to form the TZ, the membrane vesicle becomes severely deformed to embrace the elongated axoneme (Fig. 3g, left; cartoon 1), whereas the contact between distal appendages and membranes remains at the base of the cilium (red in cartoon 1). In contrast, in CEP162-depleted cells, a small membrane vesicle with an unaltered or slightly flatten shape was often seen linked peripherally through the distal appendage to centriole distal ends (22 out of 49 mature centrioles), where the outgrowth of a short ciliary bud was evident, but no signs of membrane crosslinking alongside MTs were apparent (Fig. 3g, middle & right; cartoon 2). These observations suggest that loss of CEP162 does not affect centriole-to-membrane

docking mediated by distal appendages, but instead arrests ciliogenesis at the stage of TZ assembly.

To confirm the absence of an intact TZ at CEP162-deficient centrioles, the localization of other TZ components was examined. The TZ houses several multiprotein complexes including NPHP1-4-8[15, 16], MKS/B9[13, 15, 17], and CEP290/NPHP5[15] complexes. Intriguingly, upon G0/G1 arrest, NPHP8 (or RPGRIP1L) was efficiently recruited to wild-type centrioles before cilia formed, but failed to do so in the absence of CEP162 (Fig. 3h). Consistently, CEP162-deficient centrioles failed to recruit NPHP1 (Fig. 3i), but had no problem to recruit IFT88 (Fig. 3i & d), indicating that targeting of the NPHP1-4-8 complex to the TZ depends on CEP162. Moreover, while CEP162 is not required for the localization of Tctn1 and Cc2d2a (members of MKS/B9 complex) (Fig. 3e & f), CEP162 depletion severely disrupted the recruitment of Tctn2 and TMEM67 (Fig. 3j & k), two components of MKS/B9 complex that contain the transmembrane (TM) domain[15, 17, 19]. Note that the stability or protein level of TZ components examined here is not affected by CEP162 depletion (Fig. 3l), and that these TZ deficiencies are consistent with the EM results, revealing a lack of intact TZ structures or membranes. Together, our results indicate that the microtubule-binding protein CEP162 plays a critical role in the assembly or maintenance of the ciliary transition zone.

CEP162 recognizes ciliary axonemes at the tip

We hypothesized that CEP162 recognizes and/or stabilizes ciliary MTs at centriole distal ends to promote TZ formation. To explore whether CEP162 interacts with ciliary MTs, CEP162 $^{\Delta CC3}$ and CEP162^{tNC1C2}, which are both defective in centriole tethering but retain MT-binding activity, or CEP162^{C2C3}, which lacks MT-binding activity, were inducibly expressed at a comparable level in wild-type RPE1 cells (Fig. 4a–d). Strikingly, exogenous CEP162 $^{\Delta CC3}$ (Fig. 4a) or CEP162^{tNC1C2} (Fig. 4b), but not the centriole-tethering domain CEP162^{C2C3} (Fig. 4c), strongly labeled the tips of elongated cilia, whereas endogenous CEP162 remained tethered at the cilia base (Fig. 4e). Weak labeling of CEP162^{tNC1C2} along the axoneme was also noted (Fig. 4b). Accumulation of CEP162 at cilia tips may reflect an indirect consequence of a trafficking defect in the intraflagellar transport (IFT) pathway, particularly the retrograde transport[9], caused by overexpression of truncated CEP162. To test this idea, we examined the cilia length, as most IFT defects are known to either eliminate or shorten the cilia[9]. Intriguingly, the length of cilia modified by CEP162 $^{\Delta CC3}$ was greatly enhanced rather than reduced (Fig. 4f). Moreover, higher fractions of cells with cilia were seen in proliferating populations (Fig. 4g), suggesting that overexpression of CEP162 $^{\Delta CC3}$ does not compromise IFT activity in cilia assembly. Rather, this result suggests that CEP162 recognizes and stabilizes axonemes at tips, but that this is normally restricted to distal ends of centrioles, where nascent doublet MTs grow and form the TZ.

To explore whether purified CEP162 can bind directly to the tip of membrane-extracted axonemes, wild-type RPE1 cells cultivated to form cilia were extracted with detergent-containing buffer (0.1% Triton-X100 in phosphate buffered saline). This treatment shortened but did not eliminate cilia (Fig. 4h–j), and almost completely stripped the IFT machinery off the axoneme (Fig. 4i), leaving short axonemes marked with acetylated -tubulin in nearly every ciliated cell (>80%). These membrane/IFT-extracted cilia remained attached to cells, and were incubated with different concentrations of purified CEP162 fragment (Fig. 4h). Intriguingly, whereas CEP162$^{1–227}$ did not bind to any specific cellular structure (Fig. 4h, top), low concentration of CEP162^{tNC1C2} preferentially marked cilia tips (Fig. 4h, middle). Incubation with a 10-fold higher concentration of CEP162^{tNC1C2}, but not CEP162$^{1–227}$, resulted in labeling of the entire axoneme (Fig. 4h, bottom). Furthermore, when cells expressing CEP162^{tNC1C2} were extracted with the same buffer, the tip-associated CEP162^{tNC1C2} survived the extraction, and the shortening or destabilization of cilia that

accompanies extraction of control cells was largely reduced (Fig. 4j). This indicates that CEP162 is an axoneme-recognition protein tethered at the distal end of centrioles, but when released, it can stay on axoneme tips and enhance cilia stability.

CEP162 interacts with CEP290 and mediates its association with microtubules

To determine whether CEP162 bridges TZ components to the axoneme, we examined its relationship with CEP290. CEP290 forms a complex with multiple ciliopathy molecules, including NPHP5[15], Cc2d2a, Tctn1, Mks1, and more[17], and mediates the membrane-to-MT connection in the TZ[20]. However, whether CEP290 associates directly or indirectly with ciliary MTs is unclear. Immunoprecipitation of endogenous CEP162 pulled down endogenous CEP290 (Fig. 5a), and vice versa, indicating that CEP162 and CEP290 are present in the same protein complex. Further analyses revealed that the N-terminal region of CEP162 that contains CC1 and CC2 is required to pull down endogenous CEP290 (Fig. 5b), the same region where the axoneme-binding activity resides. Endogenous CEP290 localized to the distal ends of centrioles throughout the cell cycle (Fig. 5c), and to mitotic spindles during mitosis (Fig. 5d, top), similar to CEP162. Intriguingly, CEP162 localizes to spindle MTs in the absence of CEP290 (Fig. 5d, middle), but CEP290 requires CEP162 to associate with MTs (Fig. 5d, bottom). Furthermore, overexpression of CEP162 induced MT bundles that recruited endogenous CEP290 (Fig. 5e), whereas overexpression of CEP290 failed to decorate MTs or induce MT bundles (Fig. 5f), demonstrating that CEP290 is not a MT-binding protein but associates with MTs through CEP162. Interestingly, however, the localization of CEP162 and CEP290 at centriole distal ends is independent of each other (Fig. 5g), explaining the recruitment of Ccdc2a and Tctn1 to centrioles in the absence of CEP162 (Fig. 3e & f), and further suggesting that CEP290 may serve as an anchor that recruit other TZ components to the vicinity of the TZ, whereas CEP162 is to act as a bridge to seal the gap, linking nearby TZ components to ciliary MTs.

CEP162 promotes ectopic assembly of TZ components at cilia tips

To characterize further the relationship between CEP162 and TZ assembly, we examined if CEP162 can promote ectopic assembly of TZ components. Strikingly, in cells expressing CEP162 ^{CC3} or CEP162^{tNC1C2}, several endogenous TZ components including CEP290, Tctn1, TMEM67, and NPHP8/RPGRIP1L, which are normally seen at the base of cilia, could now be found at cilia tips marked by CEP162 (Fig. 6a–d). This ectopic recruitment is specific to TZ components, as other centrosomal proteins, including CEP164 and centrin, remained localized at the cilia base under the same conditions (Fig. 6e). Thus, TZ components are targeted to an ectopic ciliary site via non-tethered CEP162, revealing CEP162 as a critical promoter for TZ assembly.

The consequence of having a TZ-like structure at cilia tips was further examined. RPE1 cells expressing GFP-tagged CEP162^{tNC1C2} were imaged by time-lapse fluorescence microscopy. The GFP-CEP162 signal was seen first at the cilia tip as expected, but surprisingly, it became detached from the tip, and released into the extracellular environment (Fig. 7a and Supplementary movie 1). In a few cases, violent bursts of cilia tips were observed (Supplementary movie 2). Similar phenotypes were also seen in cells expressing CEP162 ^{CC3}. The detached, CEP162-positive structures, scattering amongst cells, were also positive for the TZ marker CEP290 (Fig. 7b) or RPGRIP1l (Fig. 7c), IFT marker IFT88 (Fig. 7d), and ciliary membrane marker Arl13b (Fig. 7e), indicating that CEP162-modified cilia are actively discharging ciliary contents from their tips. Correlative light-scanning electron microscopy revealed that CEP162-modified tips are severely swollen (Fig. 7f), forming a blister-like configuration. The swelling is likely a consequence of excess accumulation of proteins at tips, including CEP162, and other ciliary materials (e.g. TZ components, IFT, and Arl13b). We don't understand how these ciliary materials are

excessively trapped there, although it is consistent with the idea that some form of a barrier is built, separating the tip from the rest of the ciliary compartment. The bulging structures released from cilia tips differed in size, and were irregularly shaped (Fig. 7g), suggesting that they are membranous structures randomly breaking away from the exceedingly enlarged tip. However, the GFP signal was retained over time in some of these detached structures (Supplementary Movie 1), rather than being diluted or dispersed, an indication of intact membrane-coated structures. Note that secretion-like activities have been reported to occur at the flagella tip in Chlamydomonas[32, 33]. Together, these observations demonstrate that the spatial restriction of TZ assembly to the cilia base is critical for proper cilia structure and function, and that one important role of centriole-distal-end proteins is to provide such spatial cues.

Discussion

In cycling cells, the TZ is formed transiently with most of its components recruited from the cytoplasm. However, a few TZ factors are "pre-tethered" at the assembly site, i.e. the distal end of centrioles, before ciliogenesis initiates, potentially serving as a promoter or anchor that drives TZ assembly. Our results reveal CEP162 as a critical promoter as: (a) it localizes to distal ends of centrioles, where nascent ciliary MTs form, (b) it binds directly to ciliary MTs, (c) CEP162 interacts with the core TZ component CEP290, and mediates its association with (ciliary) MTs, (d) loss of CEP162 blocks TZ assembly, and (e) gain of CEP162 at cilia tips promotes ectopic assembly of TZ components. CEP290, which localizes to centriole distal ends independent of CEP162, and anchors its associated components to the vicinity of ciliary MTs, also plays a critical role in TZ formation[15, 17, 20].

Most of centriolar components involved in ciliogenesis are concentrated at the distal portion of centrioles. Some of these factors, e.g. CEP162 and CEP290, are present at every centriole regardless of the age, but others, such as the appendages[12], associate only with mature mother centrioles. A systematic method that can differentially identify these two distinct classes of distal-end-associated molecules would greatly facilitate the study of cilia biogenesis. Here we have established a quantitative proteomic approach to map proteins associated with specific structural elements of the centrosome (Fig. 1a). This has allowed us to identify a list of molecules present at distal ends of all centrioles, and in a separate story[6], carefully characterize the molecular composition and function of the distal appendages[6]. The centriole distal end appears to play several critical roles in ciliogenesis: (i) it interacts with the membrane vesicles, which leads to docking of cilia to the plasma membrane, (ii) it is the site where ciliary microtubules grow, and (iii) it is immediately adjacent to the site of TZ assembly. It will be interesting to see if the centriole-distal-end components identified here are involved in any of these processes.

METHODS

Quantitative centrosome proteomics by SILAC Labeling Mass Spectrometry

Rational—The following two types of centrosomes were isolated from S-phase arrested cells: (i) wild-type centrosomes containing one modified centriole that is engaged with one unmodified centriole, and (ii) Plk4-induced "rosette" centrosomes[1] containing one modified centriole engaged with 4 to 6 unmodified centrioles. In both samples, only modified centrioles carry the accessory structure (i.e. PCM and appendages). Thus, the amount of any accessory protein associated only with modified centrioles should be the same between rosette and wild-type centrosomes, showing 1:1 ratio in the SILAC analysis (Fig. 1a). Importantly, non-specific contaminants co-purified with centrosomes are also present equally. Conversely, higher amounts of proteins from unmodified centrioles should associate with rosette centrosomes, showing rations higher than 1. For example, proteins

specifically associated with unmodified centrioles would give the highest ratio around 5 (5:1), while core centriolar proteins present equally in both modified and unmodified centrioles would display a smaller ratio around 3 (6:2) (Fig. 1a).

SILAC Labeling Mass Spectrometry—HeLa cells with Plk4 expression under tetracycline-inducible promoter were used in this experiment. Cells were metabolically labeled with either normal arginine and lysine or heavier isotopic variants of the two amino acids (L-Lysine 2HCL (U-13C6), L-Arginine HCL (U-13C6, U-N15N4) as previously described[22]. SILAC media was purchased from Invitrogen and prepared according to the manufacturer's recommendations. After labeling, cells in both populations were arrested in S phase by aphidicolin (Sigma), but cells fed with heavy amino acids were additionally induced to overexpress Plk4, and form rosette centrosomes. The two populations of cells were mixed and processed for centrosomes purification using the sucrose gradient centrifugation as described[2]. Centrosomes or SILAC labeled protein mixtures were run by SDS-PAGE and twelve gel sections were excised and digested overnight at pH 8.0 with modified sequencing grade trypsin (Promega Corp.). Peptide mixtures were eluted and each gel section was analyzed separately by microcapillary liquid chromatography-tandem mass spectrometry (LC-MS/MS) using the EASY-nLC nanoflow HPLC (Thermo Fisher Scientific) with a 75μm inner diameter × 15 cm length Picofrit capillary column (New Objective, Inc.) self-packed with 5μm Magic C_{18} resin (Michrom Bioresources) coupled to a hybrid LTQ Orbitrap XL-ETD mass spectrometer (Thermo Fisher Scientific). MS/MS fragmentation spectra were searched for protein identification using the Andromeda search engine (www.andromeda-search.org) against the reversed and concatenated IPI_HUMAN protein database (v3.87) (http://www.ebi.ac.uk/IPI/IPIhuman.html). One unique peptide was required for high-confidence protein identifications and a minimum ratio count of two peptides (one unique and one razor) were required for SILAC ratio determination. Normalized SILAC ratios (H/L) were used for subsequent analysis.

Cloning and Plasmids

The CEP162 cDNA was obtained from Open Biosystems. To generate HA-tagged CEP162, full-length (1–1403) or CEP162 fragments containing 1–1121, 300–1121, 617–1121, 300–956, 1–617, 617–1403, 957–1403, and 1243–1403 amino acid residues were cloned into pcDNA3-HA vector. Human CEP162 fragments containing 1–1121 and 300–1121 residues were also cloned into pEGFP-C1 to generate EGFP-CEP162 proteins. All HA- and GFP-tagged fragments were also subcloned into pLVX-tight-puro vector (Clontech) so that protein expressions can be controlled under a tetracycline-inducible promoter. To generate GST-CEP162 proteins, CEP162 fragments containing 1–227, 1–1121, and 300–1121 residues were cloned into pGEXT4T1. pEGFP-mCEP290 was obtained from Joseph Gleeson (Addgene plasmid #27379) [3].

Cell culture

HeLa, NIH3T3, and U2OS cells were cultured in DMEM medium with 10% FBS and 1% penicillin-streptomycin. Human telomerase-immortalized retinal pigment epithelial cells (hTERT-RPE1, RPE1) were cultured in DME/F-12 (1:1) medium supplemented with 10% FBS and 1% penicillin-streptomycin. Stable clones of RPE1 or HeLa cells expressing PLK4, CEP162, or CEP162 deletion mutants from the tetracycline-inducible promoter were obtained through in vivo gene delivery using the lentiviral vector pLVX-Tight-Puro vector (Clonetech). Transient transfections of plasmids into U2OS cells were performed using Lipofectamine2000 (Life Technologies).

RNAi and expression of RNAi-resistant hCEP162

Synthetic siRNA oligonucleotides were obtained from Life Technologies. Transient transfection of siRNA oligos into RPE1 cells was performed using RNAiMAX (Life Technologies). The 21-nucleotide siRNA sequences targeting CEP162 corresponded to 5'-GGTGCACCGTTGACTACTATT-3', 5'-CAACCATAGTAGTCTCGGATT-3', and 5'-GTAGCTGAACTAAATCGTATT-3'. The 21-nucleotide siRNA sequences targeting CEP290 corresponded to 5'-GATACTCGGTTTTTACGTATT-3' and 5'-CGTTGATCGACATACTAGATT-3'. The control siRNA was from Silencer® Select Negative Control No. 1 (Life Technologies). The RNAi-resistant construct (CEP162[R]) was made by introducing nucleotides changes in the targeted regions without changing the corresponding amino acids using site-directed mutagenesis (QuickChange; Agilent Technologies). The following primers were used: 5'-GTTTCTGAGCTCAACCATAGCTCCCTCGGAGTGGGATTGGACACATTA and 5'-TAATGTGTCCAATCCCACTCCGAGGGAGCTATGGTTGAGCTCAGAAAC. To generate an inducible expression system, stable clones of RPE1 cells expressing CEP162[R] from the tetracycline-inducible promoter were obtained through in vivo gene delivery.

Immunofluorescence and time-lapse microscopy

Cells were fixed with methanol at −20°C for 5 min or 4% paraformaldehyde at room temperature for 15 min. Slides were blocked with 3% bovine serum albumin (w/v) with 0.1% Triton X-100 in PBS before incubating with the indicated primary antibodies. Secondary antibodies were from molecular probes and were diluted 1:500. DNA was visualized using 4 ,6-diamidino-2-phenylindole (DAPI; Molecular Probes). Fluorescent images were acquired on an upright microscope (Axio imager; Carl Zeiss) equipped with 100× oil objectives, NA of 1.4, and a camera (ORCA ER; Hamamatsu Photonics). For time-lapse fluorescence experiments, GFP-tagged CEP162[tNC1C2] and CEP162 [CC3] were induced in hTERT-RPE1 cells and cells were imaged using a Zeiss Axiovert microscope configures with a 63X objective, motorized temperature-controlled stage, environmental chamber, and CO2 enrichment system (Zeiss, Germany). Images were acquired and processed by EMCCD camera (Hamamatsu Photonics) and axiovision software (Zeiss, Germany).

Antibodies

A rat polyclonal antibody against human CEP162 was produced using affinity purified GST-CEP162[1–227] as antigen, and used at a 1:5000 dilution. A rabbit polyclonal antibody against human C-Nap1 was produced as previous described[2]. Other antibodies used in this study include anti-CEP162 (HPA030170; 1:2000 dilution), cc2d2a (HPA044124; 1:200 dilution), RPGRIP1L (HPA039405; 1:200 dilution), OFD1 (HPA031103; 1:200 dilution), acetylated-tubulin (clone 6-11B-1, T7451; 1:2000 dilution), Flag (clone M2, F3165, 1:5000 dilution), and -tubulin (clone DM1A, T9026; 1:2000 dilution for IF; 1:5000 dilution for immunoblotting) (Sigma-Aldrich); anti-HA.11 (clone 16B12, MMS-101P; 1:1000 dilution for both IF and immunoblotting) (Covance), anti-CP110 (12780-1-AP; 1:200 dilution), IFT88 (13967-1-AP; 1:500 dilution), TCTN1(15004-1-AP; 1:200 dilution), TCTN2 (17053-1-AP; 1:200 dilution), and Tmem67(13975-1-AP; 1:100 dilution) (Proteintech); anti-centrin3 (clone 3E6, H00001070-M01; 1:200 dilution) and CEP164 (45330002; 1:5000 dilution) (Novus Biologicals); anti-CEP290 (A301-659A; 1:2000) (Bethyl laboratories, Inc), anti– -tubulin (MCA77G; 1:1000 dilution) (AbD serotec); anti-GFP-FITC (600-102-215) (Rockland); anti-NPHP1 (nephrocystin c-20, sc20204; 1:300 dilution), -tubulin (Tu30; sc-51715; 1:500 dilution) and hSAS-6 (clone 91.390.21, sc-81431; 1:200)(Santa Cruz Biotechnology, Inc.).

Immunoblotting and Immunoprecipitation (IP) experiments

Cell were lysed in NP-40 lysis buffer (50 mM Tris-HCl at PH 8.0, 150 mM NaCl. 1% NP40) with protease inhibitor for 30 min at 4°C. After centrifugation, cell lysates were resolved by SDS-PAGE and analyzed by immunoblotting using different antibodies as indicated.

For immunoprecipitation, cell lysates were incubated with rat anti-CEP162, rabbit anti-CEP290, or control IgG. The immunoprecipitates were resuspended in SDS sample buffer (50 mM Tris-HCl at PH 6.8, 2% SDS, 10% glycerol, 0.1% bromophenol blue) containing 2-mercaptoethanol, and processed for immunoblotting.

Microtubule co-sedimentation

Purified taxol-stabilized microtubules were purchase from Cytoskeleton Inc. and diluted to a final concentration of 2 mg/ml in taxol-containing BRB80 buffer (80 mM PIPES, PH 6.8, 1mM $MgCl_2$, 1mM EGTA including protease inhibitor, 1 mM GTP, 1mM DTT, and 20 μM taxol). Taxol-stabilized microtubules were mixed with CEP162 fragments affinity-purified from *E. coli*, or with cell extracts (1.5 mg protein) prepared from U2OS cells in BRB80 buffer, and pre-spun at 70000 rpm for 10 min with a TLN 100 rotor (Beckman) to remove protein aggregates and short microtubules. After 30 min of incubation at 30°C, microtubules in samples were spun through a 1.5ml cushion (40% glycerol, 1 mM GTP, ptotease inhibitor, and 20 μM taxol in BRB80) at 55000 rpm for 10 min in a TLS-55 rotor (Beckman). Both supernatants and pellets were collected and analyzed.

Zebrafish

Wild-type AB Zebrafish (*Danio rerio*) and transgenic *Tg(sox17:GFP)*[4] and *Tg(cmlc2:GFP)*[5] were obtained from the Zebrafish International Resource Center (ZIRC). Embryos were staged as described[6]. **Whole mount In situ RNA Hybridization:** PCR amplified zebrafish *cep162* cDNA was cloned into PCS2+ vector. *cep162* and *southpaw* (*spaw*)[7] cDNA constructs were used to generate *in vitro* synthesized RNA probes labeled with digoxygenenin (Roche DIG RNA labeling kit). *In situ* RNA hybridizations were performed as described[8]. **Embryo injections, reverse transcription and PCR:** Antisense morpholino oligonucleotides (MO) were obtained from Gene Tools, LLC. 2 ng of a splice-site blocking MO designed to disrupt splicing of *cep162* (5' CAGGCCACACCAGCACTCACCTTTC -3') was injected between the 1–2 cell stages to allow MO to be distributed to all embryonic cells. Cep162 MO was co-injected with 4 ng p53 MO (5'-GCGCCATTGCTTTGCAAGAATTG-3') to avoid non-specific MO effects[9]. For RT-PCR analysis of cep162 expression, total mRNA was extracted from 8 somite stage embryos using Trizol and a cDNA library was generated using iScript cDNA synthesis kit (Bio-Rad). Primers (Cep162-F: 5'-atggctcatagactgaccaaagagg -3' and Cep162-R: 5'-AATCTGGATGTTCTCCTCCTGTAAG -3') were used to amplify the N-terminus of Cep162 to determine efficacy of knockdown.

TEM

Cells grown on coverslips made of Aclar film (Electron Microscopy Sciences) were fixed in 4% paraformaldehyde and 2.5% glutaraldehyde with 0.1% tannic acid in 0.1 M sodium cacodylate buffer at room temperature for 30min, postfixed in 1% OsO_4 in sodium cacodylate buffer for 30min on ice, dehydrated in graded series of ethanol, infiltrated with EPON812 resin (Electron Microcopy Sciences), and then embedded in the resin. Serial sections (~90-nm thickness) were cut on a microtome (Ultracut UC6; Leica) and stained with 1% uranyl acetate as well as 1% lead citrate. Samples were examined on JOEL transmission electron microscope.

Correlative Light and Scanning Electron Microscopy

Cells were grown on square 22 mm coverslips, fixed for 30 minutes at RT with 4% paraformaldehyde, 2% glutaraldehyde, buffered with 0.1 M sodium cacodylate followed by 0.1% sodium borohydride to quench glutaraldehyde autofluorescense. Cells were then processed for immunofluorescence (as above). Following fluorescent staining, the cells were dehydrated through a graded ethanol series to 95% ethanol to limit quenching of florescence that occurs when exposed to 100% ethanol. Cells were placed in three changes of hexamethyldisilazane, the final change was allowed to evaporate and fully dry the cells under a fume hood. **Fluorescence Imaging:** Samples were imaged with a Zeiss AxioObserver using Zeiss Shuttle and Find. Coverslips (one at a time) were securely fastened in a Zeiss designed coverslip holder. Prior to imaging, the coverslip was calibrated using fiducial markers built into the coverslip holder to assign precise XY coordinates to targeted cells. Fluorescing cells were imaged with a 63x oil objective using Zeiss AxioVision v4.8 and captured with a Ziess HRm camera. **Scanning Electron Microscopy (SEM):** After fluorescence imaging, the coverslip holder was placed on the stage of a Zeiss SUPRA 40 Field Emission Scanning Electron Microscope (SEM). Zeiss Shuttle and Find software was again used to calibrate the stage and automatically locate the target cells. The SAME cells imaged for fluorescence were then imaged at an accelerating voltage of 3 kV. Merged SEM and color images were created using Zeiss AxioVision v 4.8.

Supplementary Material

Refer to Web version on PubMed Central for supplementary material.

Acknowledgments

Reference

1. Sorokin S. Centrioles and the formation of rudimentary cilia by fibroblasts and smooth muscle cells. The Journal of cell biology. 1962; 15:363–377. [PubMed: 13978319]

2. Sorokin SP. Reconstructions of centriole formation and ciliogenesis in mammalian lungs. Journal of cell science. 1968; 3:207–230. [PubMed: 5661997]

3. Eggenschwiler JT, Anderson KV. Cilia and developmental signaling. Annual review of cell and developmental biology. 2007; 23:345–373.

4. Rohatgi R, Snell WJ. The ciliary membrane. Current opinion in cell biology. 2010; 22:541–546. [PubMed: 20399632]

5. Schmidt KN, et al. Cep164 mediates vesicular docking to the mother centriole during early steps of ciliogenesis. The Journal of cell biology. 2012; 199:1083–1101. [PubMed: 23253480]

6. Tanos BE, et al. Centriole distal appendages promote membrane docking, leading to cilia initiation. Genes & development. 2013; 27:163–168. [PubMed: 23348840]

7. Gilula NB, Satir P. The ciliary necklace. A ciliary membrane specialization. The Journal of cell biology. 1972; 53:494–509. [PubMed: 4554367]

8. Ishikawa H, Marshall WF. Ciliogenesis: building the cell's antenna. Nature reviews. Molecular cell biology. 2011; 12:222–234.

9. Pedersen LB, Rosenbaum JL. Intraflagellar transport (IFT) role in ciliary assembly, resorption and signalling. Current topics in developmental biology. 2008; 85:23–61. [PubMed: 19147001]

10. Hu Q, et al. A septin diffusion barrier at the base of the primary cilium maintains ciliary membrane protein distribution. Science. 2010; 329:436–439. [PubMed: 20558667]

11. Kee HL, et al. A size-exclusion permeability barrier and nucleoporins characterize a ciliary pore complex that regulates transport into cilia. Nature cell biology. 2012; 14:431–437.

12. Anderson RG. The three-dimensional structure of the basal body from the rhesus monkey oviduct. The Journal of cell biology. 1972; 54:246–265. [PubMed: 5064817]

13. Chih B, et al. A ciliopathy complex at the transition zone protects the cilia as a privileged membrane domain. Nature cell biology. 2012; 14:61–72.

14. Reiter JF, Blacque OE, Leroux MR. The base of the cilium: roles for transition fibres and the transition zone in ciliary formation, maintenance and compartmentalization. EMBO reports. 2012; 13:608–618. [PubMed: 22653444]

15. Sang L, et al. Mapping the NPHP-JBTS-MKS protein network reveals ciliopathy disease genes and pathways. Cell. 2011; 145:513–528. [PubMed: 21565611]

16. Williams CL, et al. MKS and NPHP modules cooperate to establish basal body/transition zone membrane associations and ciliary gate function during ciliogenesis. The Journal of cell biology. 2011; 192:1023–1041. [PubMed: 21422230]

17. Garcia-Gonzalo FR, et al. A transition zone complex regulates mammalian ciliogenesis and ciliary membrane composition. Nature genetics. 2011; 43:776–784. [PubMed: 21725307]

18. Winkelbauer ME, Schafer JC, Haycraft CJ, Swoboda P, Yoder BK. The C elegans homologs of nephrocystin-1 and nephrocystin-4 are cilia transition zone proteins involved in chemosensory perception. Journal of cell science. 2005; 118:5575–5587. [PubMed: 16291722]

19. Czarnecki PG, Shah JV. The ciliary transition zone: from morphology and molecules to medicine. Trends in cell biology. 2012; 22:201–210. [PubMed: 22401885]

20. Craige B, et al. CEP290 tethers flagellar transition zone microtubules to the membrane and regulates flagellar protein content. The Journal of cell biology. 2010; 190:927–940. [PubMed: 20819941]

21. Wang WJ, Soni RK, Uryu K, Tsou MF. The conversion of centrioles to centrosomes: essential coupling of duplication with segregation. The Journal of cell biology. 2011; 193:727–739. [PubMed: 21576395]

22. Ong SE, et al. Stable isotope labeling by amino acids in cell culture, SILAC, as a simple and accurate approach to expression proteomics. Molecular & cellular proteomics : MCP. 2002; 1:376–386. [PubMed: 12118079]

23. Spektor A, Tsang WY, Khoo D, Dynlacht BD. Cep97 and CP110 suppress a cilia assembly program. Cell. 2007; 130:678–690. [PubMed: 17719545]

24. Singla V, Romaguera-Ros M, Garcia-Verdugo JM, Reiter JF. Ofd1, a human disease gene, regulates the length and distal structure of centrioles. Developmental cell. 2010; 18:410–424. [PubMed: 20230748]

25. Tsang WY, et al. CP110 suppresses primary cilia formation through its interaction with CEP290, a protein deficient in human ciliary disease. Developmental cell. 2008; 15:187–197. [PubMed: 18694559]

26. Otto EA, et al. Candidate exome capture identifies mutation of SDCCAG8 as the cause of a retinal-renal ciliopathy. Nature genetics. 2010; 42:840–850. [PubMed: 20835237]

27. Tsang WY, et al. Cep76, a centrosomal protein that specifically restrains centriole reduplication. Developmental cell. 2009; 16:649–660. [PubMed: 19460342]

28. Jakobsen L, et al. Novel asymmetrically localizing components of human centrosomes identified by complementary proteomics methods. The EMBO journal. 2011; 30:1520–1535. [PubMed: 21399614]

29. Leon A, Omri B, Gely A, Klein C, Crisanti P. QN1/KIAA1009: a new essential protein for chromosome segregation and mitotic spindle assembly. Oncogene. 2006; 25:1887–1895. [PubMed: 16302001]

30. Fry AM, et al. C-Nap1, a novel centrosomal coiled-coil protein and candidate substrate of the cell cycle-regulated protein kinase Nek2. The Journal of cell biology. 1998; 141:1563–1574. [PubMed: 9647649]

31. Graser S, et al. Cep164, a novel centriole appendage protein required for primary cilium formation. The Journal of cell biology. 2007; 179:321–330. [PubMed: 17954613]

32. Snell WJ. Mating in Chlamydomonas: a system for the study of specific cell adhesion. I. Ultrastructural and electrophoretic analyses of flagellar surface components involved in adhesion. The Journal of cell biology. 1976; 68:48–69. [PubMed: 1245545]

33. Baldari CT, Rosenbaum J. Intraflagellar transport: it's not just for cilia anymore. Current opinion in cell biology. 2010; 22:75–80. [PubMed: 19962875]

Additional Reference

1. Habedanck R, Stierhof YD, Wilkinson CJ, Nigg EA. The Polo kinase Plk4 functions in centriole duplication. Nature cell biology. 2005; 7:1140–1146.

2. Tsou MF, Stearns T. Mechanism limiting centrosome duplication to once per cell cycle. Nature. 2006; 442:947–951. [PubMed: 16862117]

3. Valente EM, et al. Mutations in CEP290, which encodes a centrosomal protein, cause pleiotropic forms of Joubert syndrome. Nature genetics. 2006; 38:623–625. [PubMed: 16682970]

4. Sakaguchi T, Kikuchi Y, Kuroiwa A, Takeda H, Stainier DY. The yolk syncytial layer regulates myocardial migration by influencing extracellular matrix assembly in zebrafish. Development. 2006; 133:4063–4072. [PubMed: 17008449]

5. Huang CJ, Tu CT, Hsiao CD, Hsieh FJ, Tsai HJ. Germ-line transmission of a myocardium-specific GFP transgene reveals critical regulatory elements in the cardiac myosin light chain 2 promoter of zebrafish. Developmental dynamics : an official publication of the American Association of Anatomists. 2003; 228:30–40. [PubMed: 12950077]

6. Kimmel CB, Ballard WW, Kimmel SR, Ullmann B, Schilling TF. Stages of embryonic development of the zebrafish. Developmental dynamics : an official publication of the American Association of Anatomists. 1995; 203:253–310. [PubMed: 8589427]

7. Long S, Ahmad N, Rebagliati M. The zebrafish nodal-related gene southpaw is required for visceral and diencephalic left-right asymmetry. Development. 2003; 130:2303–2316. [PubMed: 12702646]

8. Gao C, Wang G, Amack JD, Mitchell DR. Oda16/Wdr69 is essential for axonemal dynein assembly and ciliary motility during zebrafish embryogenesis. Developmental dynamics : an official publication of the American Association of Anatomists. 2010; 239:2190–2197. [PubMed: 20568242]

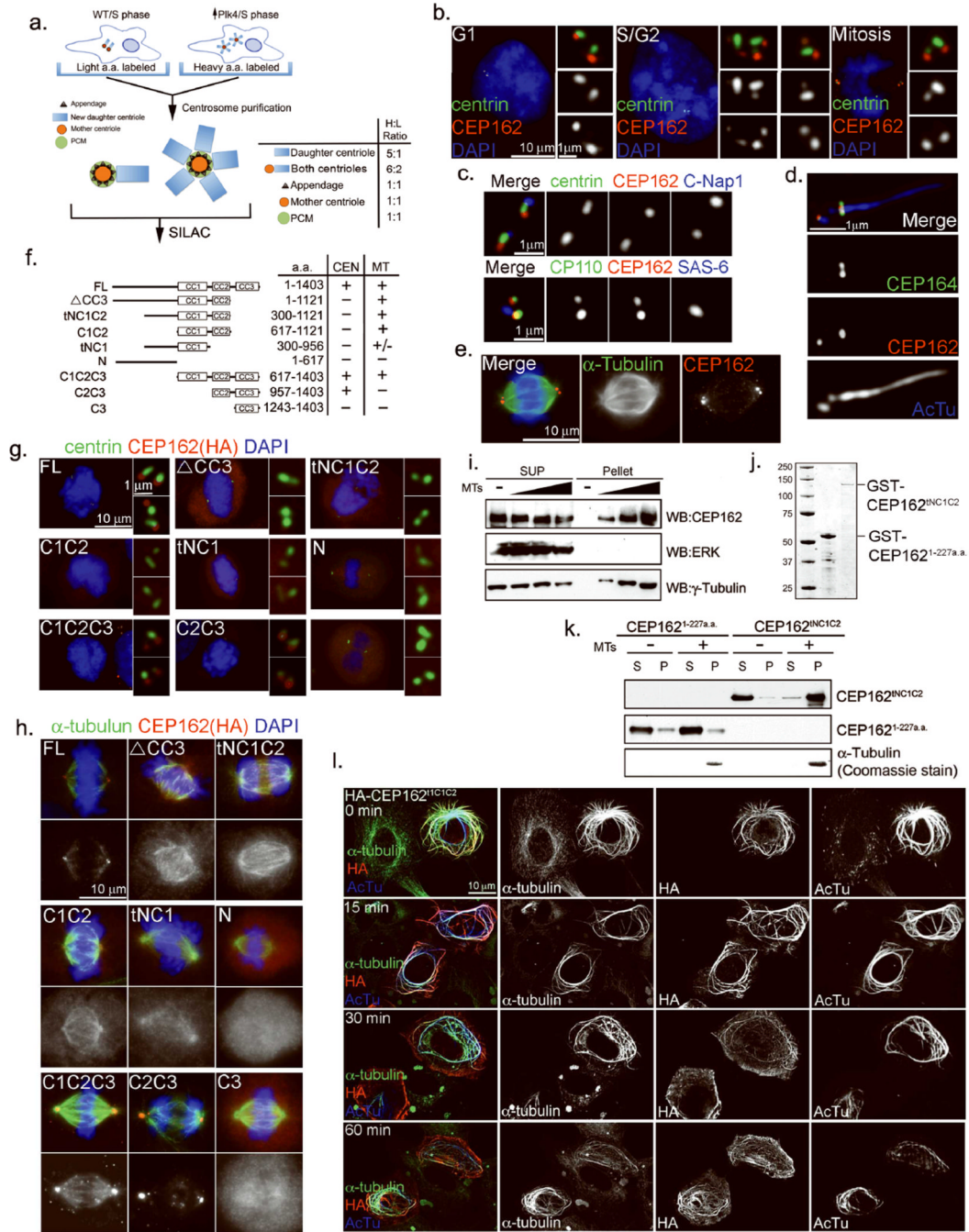9. Robu ME, et al. p53 activation by knockdown technologies. PLoS genetics. 2007; 3:e78. [PubMed: 17530925]

Figure 1. Identification of CEP162 as a MT-binding protein localized at centriole distal ends
a, Schematic outline of the SILAC-based proteomic analysis carried out to quantitatively
dissect the centrosome proteome (see Suppl. Methods for details). Core centriolar proteins
localizing to both mother and newly formed daughter centrioles give a higher H/L ratio (6:2)
than mother centriole specific proteins (1:1). **b,** CEP162 is present at centrioles throughout
the cell cycle. RPE1 cells in different cell cycle stages were processed for
immunofluorescence with indicated antibodies. Nuclei were visualized with DAPI (blue). **c,**
CEP162 (red) localizes to the distal end of centrioles, in comparison to other centriole
markers as indicated. **d**, CEP162 (red) localizes to the region between centrioles and

axonemes (blue) in RPE1 cells, surrounded by CEP164 (green). AcTu: anti-acetylated - tubulin. **e**, CEP162 (red) decorates spindle microtubules (green). DNA (DAPI, blue). **f**, Domain analyses of CEP162 for its microtubule binding (MT) and centriolar localization (CEN). **g, h,** The binding of CEP162 to centrioles and microtubules are separable. RPE-1 cells expressing HA-tagged fragments of CEP162 as indicated were stained with antibodies indicated. DNA (DAPI, blue). **i**, Endogenous CEP162 binds to microtubules. U2OS cell extracts were incubated with increasing amounts of taxol-stabilized microtubules (MTs) and then centrifuged (55000rpm, 10min) to form supernatant (S) and pellet (P) fractions. Samples from both fractions were probed with antibodies indicated. ERK and -tubulin were used as negative and positive controls for MT binding respectively. **j**, Coomassie blue stains of GST-CEP162$^{aa1-227}$ and GST-CEP162^{tNC1C2} fusion proteins purified from *E. coli*. **k**, A MT-pelleting assay. Purified CEP162^{tNC1C2}, but not CEP162$^{1-227}$, fused with glutathione S-transferase (GST) was co-pelleted with taxol-stabilized microtubules (MTs). CEP162 was probed by anti-CEP162 antibodies; pelleted microtubules were detected by coomassie blue staining. **l**, Overexpression of CEP162^{tNC1C2} induces MT bundles. U2OS cells transiently expressing HA-tagged CEP162^{tNC1C2} were cold treated for indicated amounts of time, and stained with indicated antibodies Uncropped images of all immunoblots are presented in Supplementary Fig. S1.
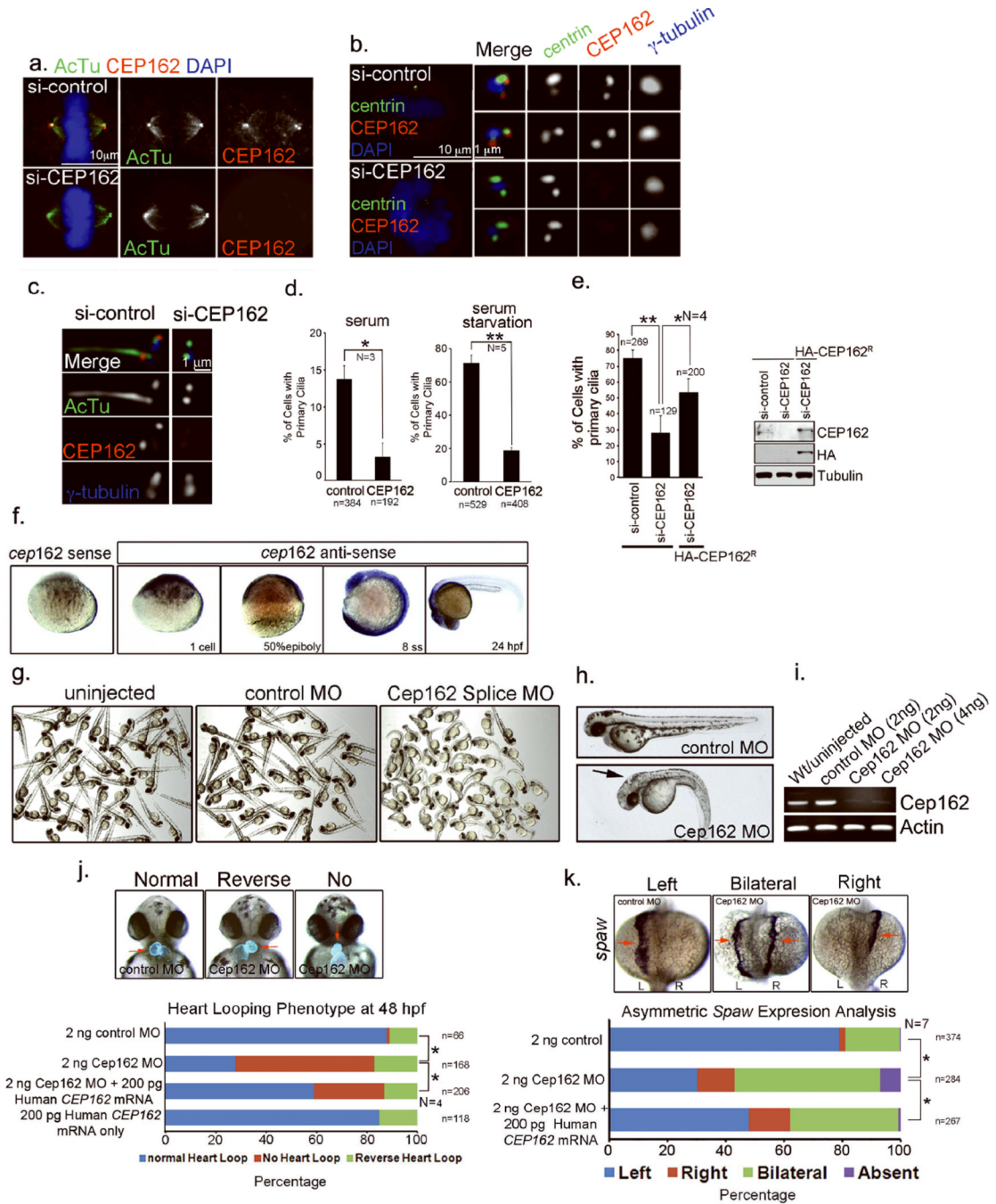
Figure 2. CEP162 is required for ciliogenesis
a–c, RPE1 cells transfected with control or CEP162 siRNA for 96hr were stained with antibodies indicated. **d**, Effects of CEP162 depletion on cilia formation in proliferating (left) or G0-arrested (right) cells were quantified from 3 or 5 independent experiments as indicated. Error bars represent standard deviation (SD). The significance (two-tailed *t*-test) is indicated, *P < 0.05, **P < 0.001. **e,** Cilia defects in RPE1 cells were rescued by expressing HA-tagged, RNAi-resistant form of CEP162 (CEP162^R). Error bars indicate standard deviation (SD). The significance (two-tailed *t*-test) is indicated, *P < 0.05, **P < 0.001, N = 4. The protein level of CEP162 in different experimental conditions was shown. Uncropped

images of immunoblots are presented in Supplementary Fig. S1. **f,** In zebrafish embryos, whole mount RNA *in situ* hybridizations revealed *cep162* mRNA is maternally loaded at the 1-cell stage and then ubiquitously expressed at the 50% epiboly stage and 8 somite stage (ss). At 24 hours post-fertilization (hpf), Cep162 is highly expressed in the head region. A control *cep162* sense probe was used to determine probe specificity. **g & h**, Morphology of zebrafish embryos at 2 days post-fertilization injected with either control or Cep162 morpholinos (MO) at the one-cell stage. Cep162 MO injected embryos showed body axis defects, hydeocephalus (arrow) and altered left-right asymmetric heart looping. **i,** RT-PCR showed that levels of correctly spliced *cep162* mRNA were significantly reduced in Cep162 knockdown embryos. Loading control: actin. **j,** Cep162 MO embryos showed an altered left-right asymmetric heart looping. Transgenic *Tg(cmlc2:GFP)* embryos that express GFP specifically in the heart (red arrows) were used to visualize heart looping. In control embryos the heart looped to the right, whereas Cep162 MO knockdown often resulted in reversed or no heart looping. Human *CEP162* mRNA partially rescued these heart looping defects. Data were collected from 4 independent experiments (N = 4). The significance (*One-way ANOVA and pos- hoc test*) is indicated, $^{*}P < 0.05$. **k,** Left-right asymmetry defects were observed when RNA *in situ* hybridization analysis of spaw expression, which is normally detected in left lateral plate mesoderm at 14 hours post-fertilization, but was often found to be bilateral or right-sided in Cep162 MO injected embryos. Co-injecting Cep162 MO with human *CEP162* mRNA partially rescued *spaw* defects. Data were collected from 7 independent experiments (N = 7). The significance (*One-way ANOVA and pos- hoc test*) is indicated, $^{*}P < 0.05$. L=left; R=right. Total cell counts are shown on the figures (as n). Sample size for each independent experiment: n>50 (d), n>25 (e), n>15 (j & k) were analyzed for each independent experiment I; Table S1 presents the source data for the graphs
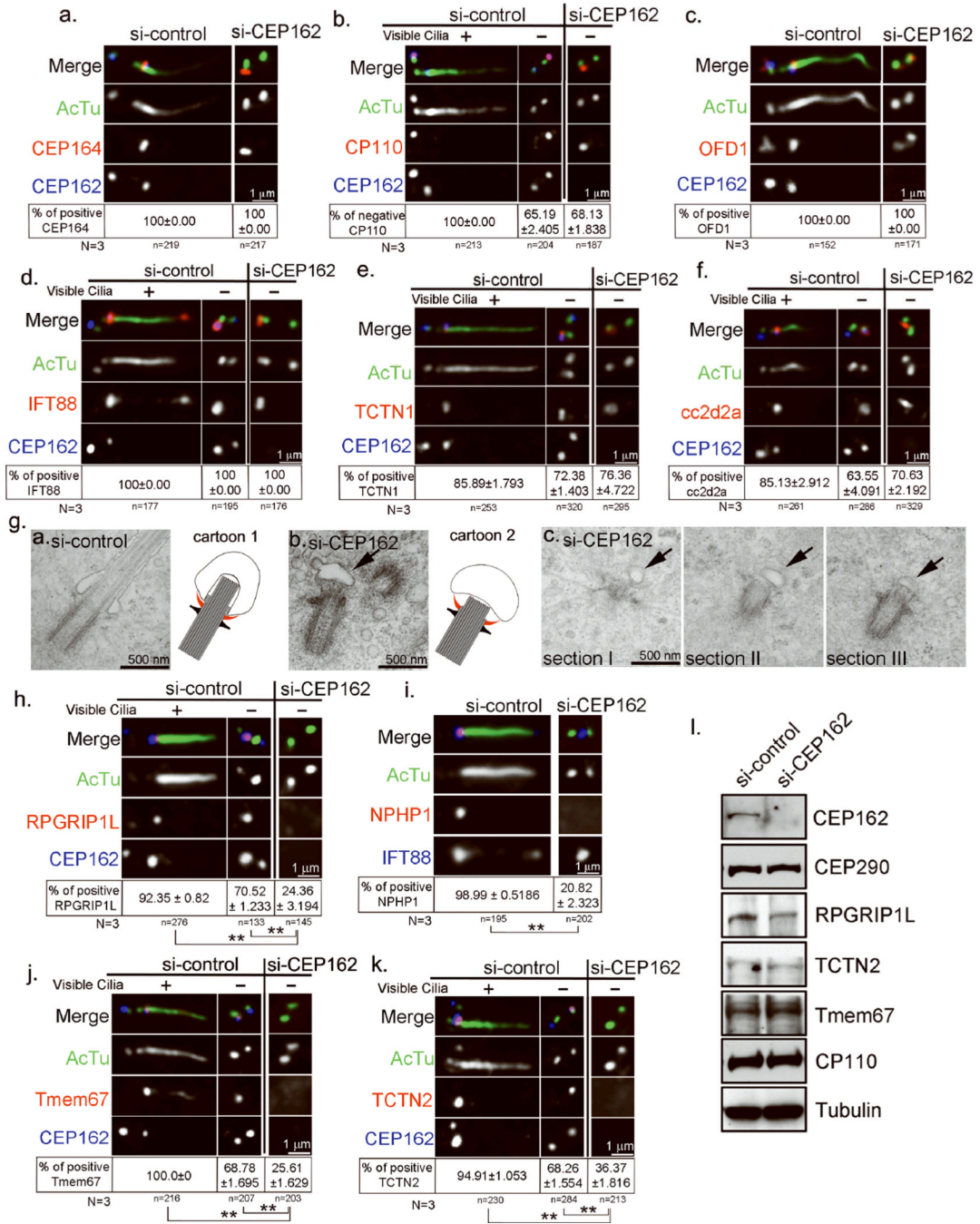
Figure 3. Loss of CEP162 blocks ciliogenesis at the stage of TZ assembly
a–f, RPE1 cells transfected with control or CEP162 siRNA followed by serum starvation for 48 hours were stained with antibodies indicated. Only G1 cells that contain two un-duplicated centrioles were scored. In some controls (**b, & d-f**), both ciliated and non-ciliated G1 cells were shown. Note that the removal of CP110 (**b**), or the recruitment of IFT88 (**d**), TCTN1 (**e**), and cc2d2a (**f**) occur at wild-type centrioles before cilia formed, as well as at CEP162-deficient centrioles where cilia failed to form. Data were collected from 3 independent experiments. The percentage of cells showing the presence or absence of indicated marker at centrioles was indicated (mean ± SD). No significant differences were

detected between control and CEP162 depleted cells. **g,** TEM images of basal bodies in RPE1 cells transiently transfected with control (left) or CEP162 (middle & right) siRNA, followed by 48hr serum starvation for cilia formation. Serial sections of a basal body (right) in CEP162 knockdown cell were shown in addition to the single-sectioned image (middle). Arrows indicate small membrane vesicles connected to CEP162-deficient centrioles through the distal appendage. Schematic diagrams summarizing the phenotype were shown. Gray links: Membrane-to-MT connections; red: membrane-to-appendage connections. **h–k,** Control or CEP162-depleted RPE1 cells as described in **d–f** were examined for the presence of indicated TZ components (red). Data were collected from 3 independent experiments (N=3), and mean% ± SD% was shown. The significance (two-tailed t-test) is indicated, $^*P < 0.05$, $^{**}P < 0.001$. **l,** The protein levels of indicated TZ components were examined in control or CEP162-depleted RPE1 cells by western blot. Uncropped images of immunoblots are presented in Supplementary Fig. S1. Total cell counts are shown on the figures as n). More than 40 cells were analyzed for each independent experiment. Table S1 presents the source data for the graphs.
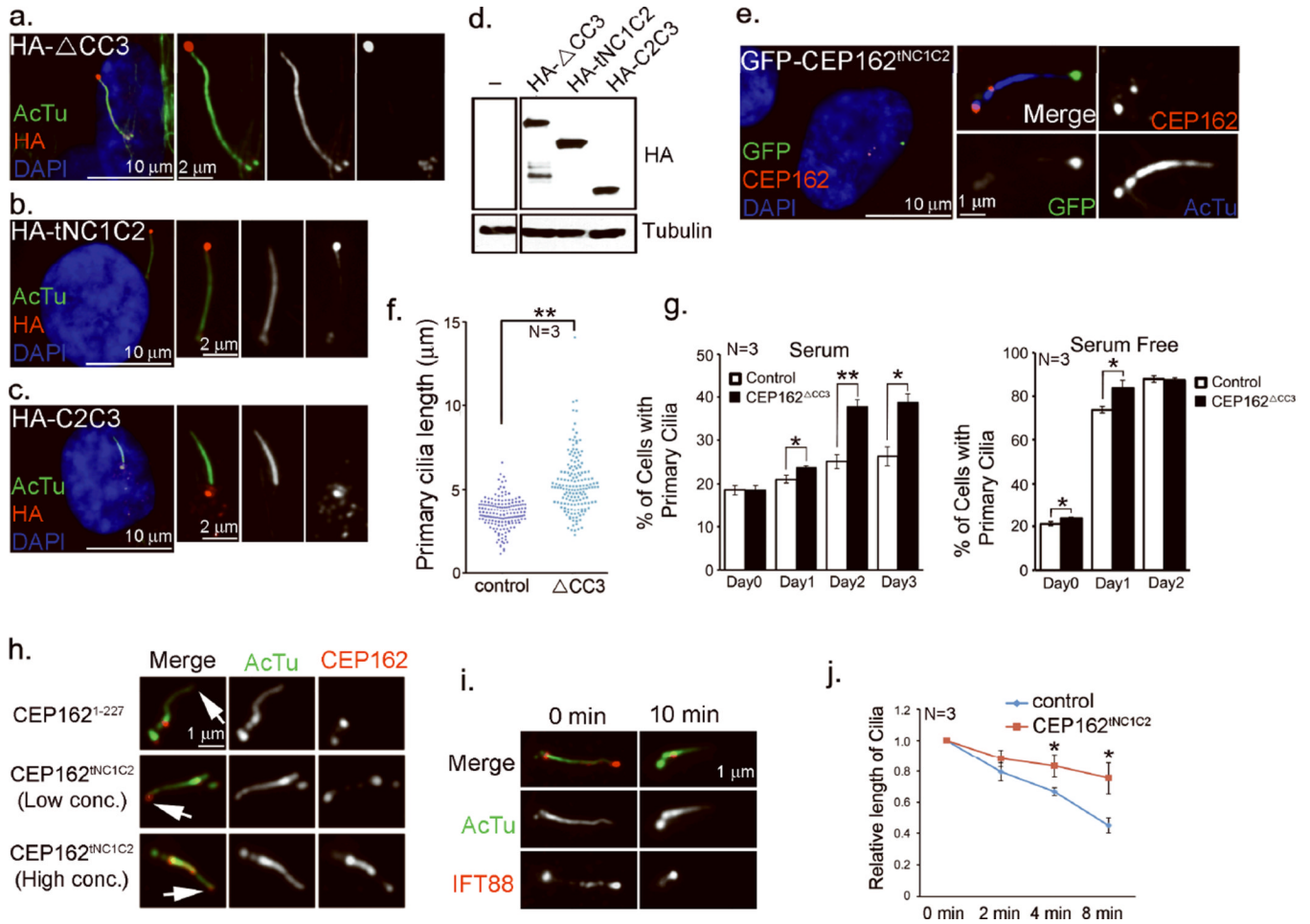
Figure 4. CEP162 is tethered at centriole distal ends to recognize axonemes

a–c, RPE1 cells expressing HA-tagged CEP162 $^{\triangle CC3}$, CEP162^{tNC1C2} or CEP162^{C2C3} as indicated were stained with anti-acetylated-tubulin (AcTu, green), anti-HA (red) and DAPI (DNA, blue). **d,** The expression levels of various deletion mutants of CEP162 were examined by western blot. Uncropped images of immunoblots are presented in Supplementary Fig. S1. **e,** Endogenous CEP162 in RPE1 cells expressing GFP-tagged CEP162^{tNC1C2} (green) was stained with rat antibodies against a N-terminal fragment (1–227 a.a.) of CEP162 (red), and anti-AcTu (blue). **f,** RPE1 cells expressing HA-tagged CEP162 $^{\triangle CC3}$ were serum starved for 48 hours to induce cilia formation. Cilia lengths were measured in μm. The significance (two-tailed t-test) is indicated, $^{**}P < 0.001$. Data were collected from 3 independent experiments (N=3). **g,** Proliferating or serum starved RPE1 cells expressing HA-tagged CEP162 $^{\triangle CC3}$ at day 0 were examined for their ciliation status at indicated time points. Data were collected from 3 independent experiments (N=3). Error bars represent standard deviation (SD). The significance (two-tailed t-test) is indicated, $^{*}P < 0.05$, $^{**}P < 0.001$. **h, i,** Demembranated axonemes, prepared from ciliated RPE1 cells treated with the extraction buffer (0.1% Triton X-100 in phosphate buffer saline) for 10 min, were either incubated with purified CEP162 fragments as indicated (**h**, red), or stained with indicated antibodies (**i**, IFT88 in red; acetylated -tubulin in green). Cilia tip are marked by arrowhead. **j,** Primary cilia in control (blue) or CEP162^{tNC1C2}-expressing cells (red) were treated with the extraction buffer for indicated time, and their average lengths relative to that of untreated (0 min) were measured at different time points. Data were collected from 3 independent experiments (N=3). Error bars indicate standard error of the mean (s.e.m.). The

significance (two-tailed *t*-test) is indicated, *P < 0.05, **P < 0.001. Sample size for each independent experiments: n>90 (g), n>50 (j) were analyzed for each independent experiment. . Table S1 presents the source data for the graphs.
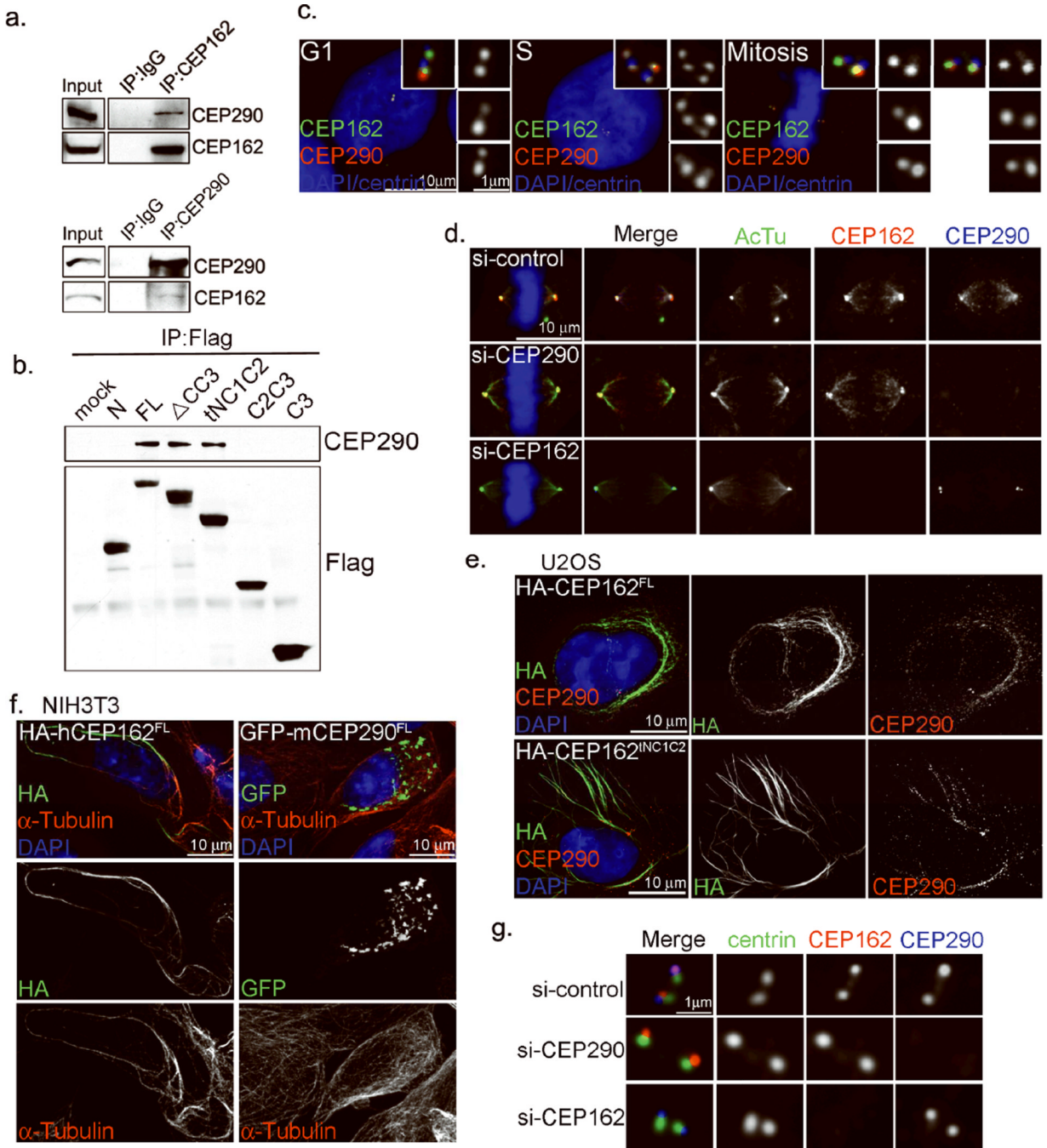
Figure 5. CEP162 interacts with CEP290 and mediates its association with MTs
a, Endogenous CEP162 or CEP290 in HEK293T cell extracts were immunoprecipitated, and co-precipitated proteins were probed with indicated antibodies by western blot. Uncropped images of immunoblots are presented in Supplementary Fig. S1. **b**, Mapping the CEP290 binding domain of CEP162. 293T cells expressing various Flag-tagged fragments of CEP162 were subjected to immunoprecipitations and western blot with antibodies as indicated. Uncropped images of immunoblots are presented in Supplementary Fig. S1. **c**, RPE1 cells at different cell cycle stages were processed for immunofluorescence with anti-CEP290 (red), anti-CEP162 (green), and anti-centrin (blue) antibodies. DNA (DAPI, blue).

d, Spindle association of CEP290 depends on CEP162. RPE1 cells transfected with control, CEP162, or CEP290 siRNA for 72 hours were stained with indicated antibodies against acetylated-tubulin (green), CEP162 (red), and CEP290 (blue). DNA (DAPI, blue). **e**, Overexpression of CEP162 induced MT bundles recruiting endogenous CEP290. U2OS cells transiently expressing HA-tagged CEP162^{FL} or HA-tagged CEP162^{tNC1C2} were stained with antibodies against CEP162 (green), CEP290 (red) and DAPI (DNA, blue). **f**, Overexpression of CEP162 but not CEP290 induced MT bundles. NIH3T3 cells transiently expressing HA-tagged human CEP162^{FL} or GFP-tagged mouse CEP290^{FL} were stained with antibodies against -tubulin (Red), CEP162 (HA, green) or CEP290 (GFP, green). **g**, Centriolar localizations of CEP290 and CEP162 are independent of each other. RPE1 cells were transfected with control, CEP162, or CEP290 siRNA for 96 hours. Cells were stained with anti-centrin (green), anti-CEP162 (red), and anti-CEP290 (blue) antibodies.
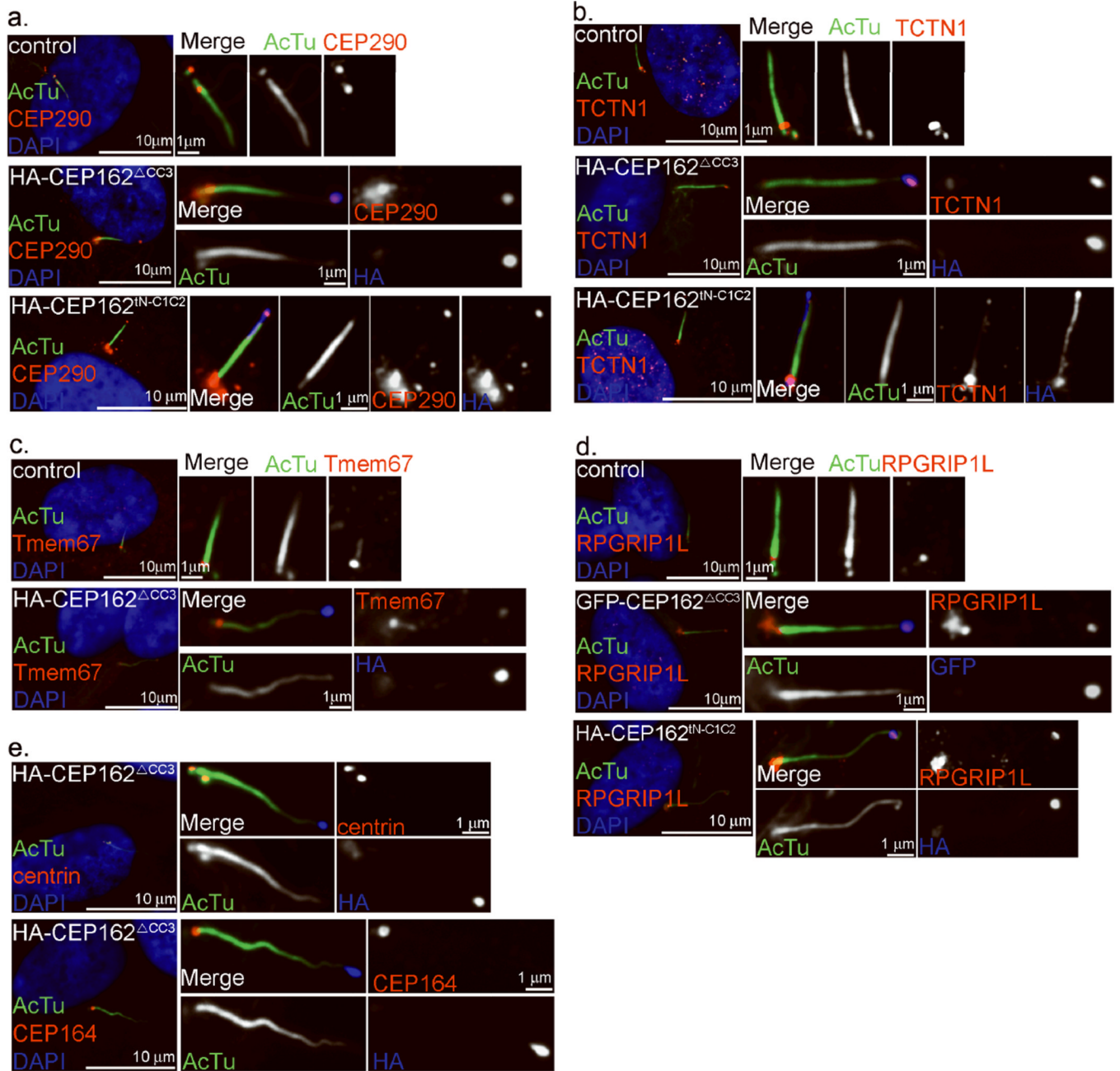
Figure 6. Untethered CEP162 promotes ectopic recruitments of TZ components to cilia tips
a–d, Ectopic recruitments of TZ components via CEP162 ^{CC3} and CEP162^{tNC1C2}. HA- or GFP-tagged CEP162 ^{CC3} or CEP162^{tNC1C2} was expressed in RPE1 cells followed by serum starvation for 48hr and stained with antibodies against CEP290 (**a**), TCTN1 (**b**), Tmem67 (**c**) or RPGRIP1L (**d**) in red, acetylated-tubulin (AcTu, green) and HA (blue). Nuclei were visualized with DAPI (blue). **e**, Centriole-bound components, centrin (top) and CEP164 (bottom), remained localized at the cilia base in CEP162 ^{CC3}-expressing cells.
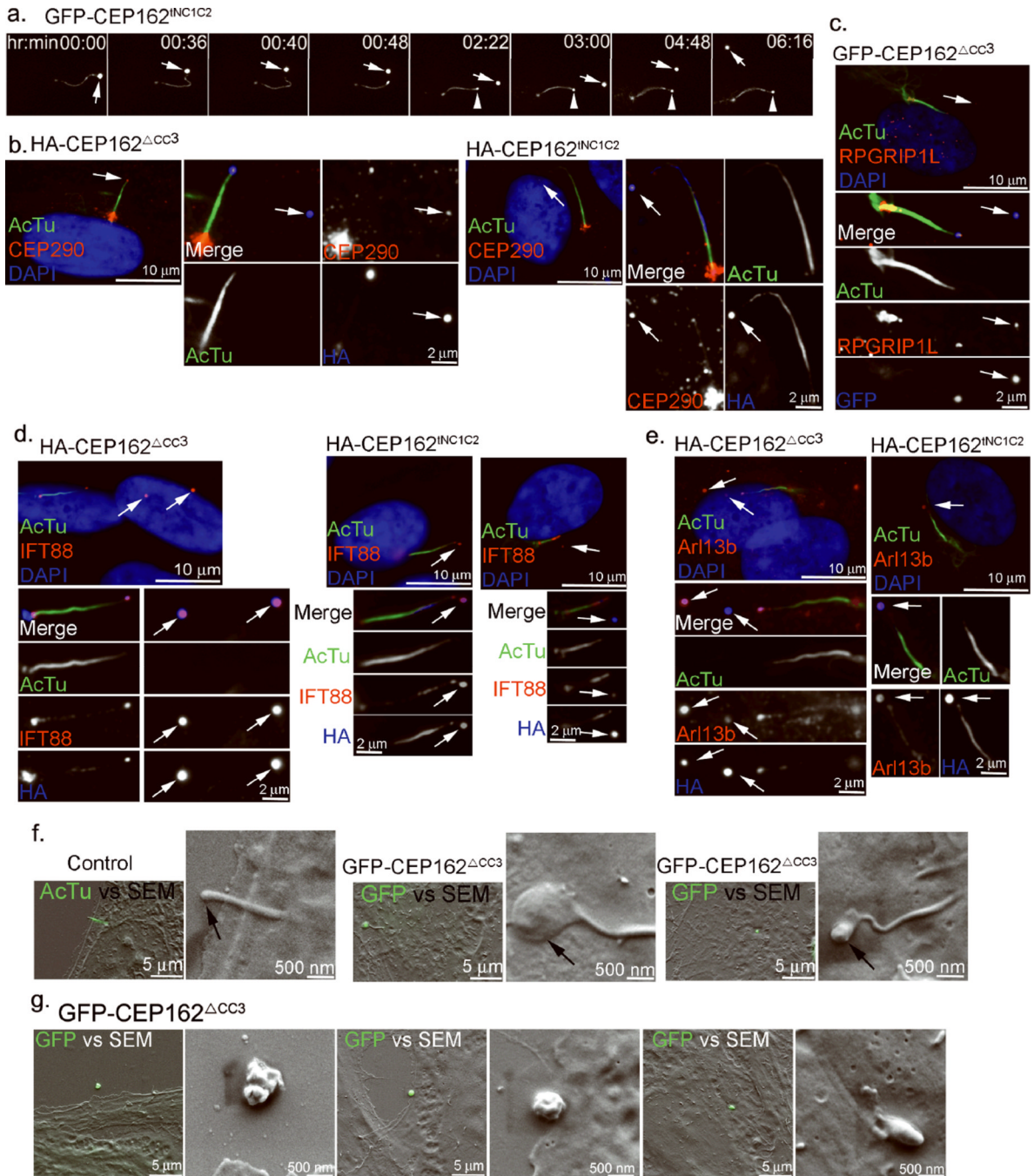
Figure 7. Cilia tips modified by CEP162 swell exceedingly and discharge ciliary contents
a, RPE1 cells expressing GFP-tagged CEP162^{tNC1C2} were traced by time-lapse fluorescence microscopy. Images were taken at 2-min time interval. Existing cilia tips were marked by arrows, and newly formed tips were marked with arrowheads. **b–e**, HA- or GFP-tagged CEP162 ^{CC3} or CEP162^{tNC1C2} was conditionally expressed in RPE1 cells followed by serum starvation for 48hr. Cells were stained with antibodies against CEP290 (**b**), RPGRIP1L (**c**), IFT88 (**d**), Arl13b (**e**) in red, acetylated-tubulin (green) and HA (blue). DNA was stained with DAPI. Arrows indicate the CEP162-positive structures released from cilia tips. **f**, Correlative light-scanning electron microscopy images of control cells (left), or

RPE1 cells expressing GFP-tagged CEP162 [CC3] (middle & right). GFP-CEP162 [CC3] (green) marked cilia tip (middle & right). Primary cilia in control cells (left) were labeled with acetylated-tubulin (green). Arrows indicate cilia tips. Merged images were shown under low SEM magnification. **g**, Correlate LM-SEM images of the swollen structure released from cilia tips in RPE1 cells expressing GFP-tagged CEP162 [CC3]. Released structures from cilia tip were marked with GFP (green). Merged images were shown under low SEM magnification.